HHS Public Access

Author manuscript

Cell Rep. Author manuscript; available in PMC 2016 June 24.

Published in final edited form as:

Cell Rep. 2015 July 14; 12(2): 326–334. doi:10.1016/j.celrep.2015.06.029.

Glutamate receptor modulation is restricted to synaptic microdomains

Gyorgy Lur and **Michael J. Higley**

Department of Neurobiology, Program in Cellular Neuroscience, Neurodegeneration and Repair, Kavli Institue, Yale School of Medicine, New Haven, CT 06510

Summary

A diverse array of neuromodulators governs cellular function in the prefrontal cortex (PFC) via the activation of G protein-coupled receptors (GPCRs). However, these functionally diverse signals are carried and amplified by a relatively small assortment of intracellular second messengers. Here, we examined whether two distinct $G\alpha_i$-coupled neuromodulators (norepinephrine and GABA) act as redundant regulators of glutamatergic synaptic transmission. Our results reveal that, within single dendritic spines of layer 5 pyramidal neurons, alpha-2 adrenergic receptors (α2Rs) selectively inhibit excitatory transmission mediated by AMPA-type glutamate receptors while Type B GABA receptors ($GABA_BRs$) inhibit NMDA-type receptors. We show that both modulators act via the downregulation of cAMP and PKA. However, by restricting the lifetime of active $G\alpha_i$, RGS4 promotes the independent control of these two distinct target proteins. Our findings highlight a mechanism by which neuromodulatory microdomains can be established in subcellular compartments such as dendritic spines.

Graphical Abstract

Correspondence: m.higley@yale.edu.

Author contributions

G.L and M.J.H. designed and performed the experiments, analyzed the data and wrote the paper.

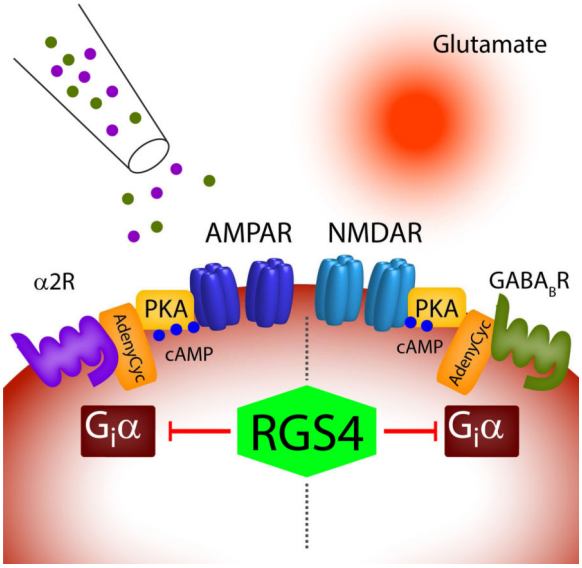

Introduction

Neuromodulation via G protein-coupled receptors (GPCRs) provides a ubiquitous mechanism for regulating neuronal activity in the mammalian brain. In contrast to classical neurotransmitters that directly excite or inhibit postsynaptic neurons, neuromodulators alter neuronal excitability and modify synaptic transmission (Destexhe et al., 1994, Dismukes, 1979). Interestingly, there is a paradoxical mismatch between the diversity of modulatory ligands and the relative paucity of GPCR-linked second messenger systems such as adenylate cyclase and phospholipase C. The mobility of dissociated G protein subunits and downstream molecules such as calcium (Ca2+), cAMP, and inositol-1,4,5-triphosphate should further reduce the cellular capacity for segregated signaling pathways. Nevertheless, there is evidence for the functional compartmentalization of soluble messengers into independent microdomains, which could contribute to neuromodulatory specificity. For example, rapid intracellular buffering coupled with potent extrusion mechanisms spatially restricts Ca2+ within presynaptic terminals and dendritic spines (Higley and Sabatini, 2008, Lisman et al., 2007, Yuste et al., 2000). However, the potential for mobile, non-ionic signaling molecules to be isolated within synaptic microdomains is largely unknown.

In the prefrontal cortex (PFC), neuromodulation by both norepinephrine (NE) and gamma-amino butyric acid (GABA) regulates higher cognitive functions, including attention and short-term “working” memory (Gamo and Arnsten, 2011, Kesner and Churchwell, 2011). Altered levels of NE and GABA are also linked to neuropsychiatric disorders, such as schizophrenia, attention deficit and addiction (Arnsten, 2011, Tyacke et al., 2010, Stan and Lewis, 2012). Experimental evidence suggests that both Type 2 alpha adrenergic receptors (α2Rs) and Type B GABA receptors (GABA$_B$Rs) modulate excitatory glutamatergic signaling in the PFC (Chalifoux and Carter, 2010, Ji et al., 2008, Liu et al., 2006). Additionally, ultrastructural studies have localized both α2Rs and GABA$_B$Rs to dendritic spines, the location of synaptic glutamate receptors (Kulik et al., 2003, Wang et al., 2007).

Both α2Rs and $GABA_BRs$ are GPCRs coupled to the G protein subunit $G\alpha_i$, whose activation leads to the inhibition of adenylate cyclase and decreased production of cAMP (Knight and Bowery, 1996, Summers and McMartin, 1993). The subsequent reduction in cAMP-dependent protein kinase (PKA) activity provides a potential mechanism for the control of both AMPA- and NMDA-type glutamate receptors (AMPARs and NMDARs, respectively) (Chen et al., 2008, Esteban et al., 2003, Raymond et al., 1994). These observations raise the question of whether α2Rs and $GABA_BRs$ act as redundant modulators of prefrontal synaptic transmission.

To test this hypothesis, we combined electrophysiological recordings and 2-photon imaging of PFC pyramidal neurons with optical stimulation of excitatory glutamatergic synapses using focal glutamate uncaging (Carter and Sabatini, 2004). Our results reveal the surprising observation that activating α2Rs reduces AMPAR-mediated responses, whereas activating $GABA_BRs$ decreases NMDAR-mediated responses. Notably, both modulatory pathways utilize $G\alpha_i$-mediated down-regulation of cAMP and PKA signaling, and this dissociation occurs despite functional evidence that both α2Rs and $GABA_BRs$ are located in the same dendritic spines. We further find that inhibiting the GTPase activating protein RGS4 eliminates the selective compartmentalization of adrenergic and GABAergic actions. Thus, RGS4 promotes the independent control of two distinct target proteins by eliminating cross-talk between signaling pathways in dendritic spines. Our results highlight a mechanism by which biochemical multiplexing can occur in subcellular microdomains.

Results

Distinct $G\alpha_i$-coupled agonists differentially modulate postsynaptic glutamate receptors

We investigated whether two distinct neuromodulators that target the same biochemical pathway produce similar changes in glutamatergic transmission. To identify the actions of α2Rs and $GABA_BRs$ on postsynaptic glutamatergic signaling, we used 2-photon laser uncaging of glutamate (2PLU) to stimulate single excitatory synapses on prefrontal L5 pyramidal neurons while recording excitatory postsynaptic currents (uEPSCs) and imaging postsynaptic calcium (Ca2+) signals. Uncaging power was individually calibrated for spines on the proximal basal dendrites (<100 μm from the soma) to emulate endogenous glutamate release from a single presynaptic terminal (Fig. 1A, S1).

First, we pharmacologically isolated AMPAR-mediated responses and recorded synaptic currents (Fig. 1B, see Methods). Bath application of the α2R agonist guanfacine (40 μM) reduced uEPSCs from 17.2 ± 0.9 pA (n=32 spines) to 8.8 ± 0.7 pA (n=32 spines, $p<0.0001$, unpaired t-test). In contrast, the $GABA_BR$ agonist baclofen (5 μM) had no effect on AMPAR-mediated uEPSC amplitude (16.9 ± 1.0 pA, n=26 spines vs. 16.9 ± 1.1 pA, n=30 spines, p=0.97). We then performed converse experiments in which we isolated NMDAR-mediated responses and recorded both uEPSCs and ΔCa2+ in the spine head (Fig. 1C,D, see Supplemental Methods). Under these conditions, 2PLU-evoked ΔCa2+ is mediated by influx through NMDARs (Fig. S2). Guanfacine had no effect on either uEPSC amplitude (24.1 ± 3.1 pA, n=38 spines, vs. 26.6 ± 2.9 pA, n=32 spines, p=0.56) or ΔCa2+ (0.71 ± 0.035 $\Delta G/G_{sat}$ vs. 0.64 ± 0.034 $\Delta G/G_{sat}$, p=0.17). In contrast, baclofen significantly reduced NMDAR-mediated ΔCa2+ in the spine head (0.68 ± 0.03 $\Delta G/G_{sat}$, n=33 spines vs. 0.49

± 0.02 $\Delta G/G_{sat}$, n=35 spines, p<0.0001) but did not alter uEPSCs (24.3 ± 2.5 pA, vs. 23.2 ± 2.0 pA, p=0.73). Thus, our results demonstrate that α2Rs and $GABA_B$Rs selectively modulate postsynaptic AMPARs and NMDARs, respectively.

Modulation of AMPARs and NMDARs is mediated by downregulation of PKA

One explanation for our results is that adrenergic and GABAergic modulation of glutamate receptors occurs via distinct biochemical signaling pathways. We therefore isolated AMPAR-mediated synaptic responses and tested the ability of H89 (10 μM), a selective blocker of cAMP-dependent kinase (PKA), to mimic and occlude the actions of guanfacine. In the presence of H89, uEPSC amplitude was 12.4 ± 1.3 pA (n=30 spines, Fig. 2A, B). In the combined presence of H89 and guanfacine, uEPSC amplitude was 9.0 ± 0.6 pA (n=35 spines, Fig. 2A, B). We also examined the actions of the selective PKA activator and cAMP analog N6-benzo-cAMP (bcAMP, 100 μM). In the presence of bcAMP, uEPSC amplitude was 19.1 ± 1.7 pA (n=30 spines). Combined application of bcAMP and guanfacine produced a uEPSC amplitude of 17.0 ± 1.5 pA (n=31 spines). A one-way ANOVA comparing all groups revealed significant differences (F=19.57, p<0.0001) that we explored using post hoc comparisons (significant for p<0.05, Tukey's test). These analyses revealed that H89 both mimicked and occluded the actions of guanfacine, whereas bcAMP blocked the actions of guanfacine (Fig. 2A, B).

In a parallel set of studies, we isolated NMDARs and examined the biochemical mechanisms underlying their modulation by baclofen. In the presence of H89, the NMDAR-mediated uEPSC was 14.8 ± 1.8 pA (n=29 spines) and the ΔCa2+ was 0.37 ± 0.03 $\Delta G/G_{sat}$. Co-application of H89 and baclofen yielded a uEPSC of 15.3 ± 1.9 pA (n=29 spines) and a ΔCa2+ of 0.36 ± 0.02 $\Delta G/G_{sat}$. After bcAMP, the uEPSC was 21.0 ± 1.6 pA and ΔCa2+ was 0.61 ± 0.03 $\Delta G/G_{sat}$ (n=30 spines), while combined bcAMP and baclofen produced a uEPSC of 28.0 ± 2.8 pA and a ΔCa2+ of 0.59 ± 0.02 $\Delta G/G_{sat}$ (n=31 spines, Fig 2C-F). As above, Tukey's post-hoc tests (ANOVA, F=43.48, p<0.0001) revealed that H89 occluded and bcAMP blocked the actions of baclofen on NMDAR-mediated responses (Fig. 2C-F).

Our data indicate that both α2Rs and $GABA_B$Rs exert control of glutamate receptors via a downregulation of PKA signaling. Phosphorylation of the Serine 845 (S845) residue of the GluA1 subunit is known to regulate AMPA-receptor stability and membrane trafficking (Esteban et al., 2003). We therefore probed whether guanfacine or baclofen altered S845 phosphorylation. Assays were performed on 4-6 independent samples, and one-way ANOVA revealed significant effects (F=19.81, p<0.0001) that were investigated with post-hoc analyses (Fig. 3A,B). In comparison to untreated PFC tissue, 10 minute incubation with either guanfacine or H89 significantly reduced S845 phosphorylation, while baclofen had no effect. In addition, the adenylate cyclase activator forskolin (50 μM) significantly increased the phosphorylation of AMPARs relative to control.

A recent study identified a PKA phosphorylation site on the GluN2B subunit, Serine 1166 (S1166), which modulates the Ca2+ permeability of NMDARs (Murphy et al., 2014). In keeping with our Ca2+ imaging data, we found that application of either baclofen or H89, but not guanfacine, reduced S1166 phosphorylation. Conversely, forskolin enhanced the phosphorylation of the same residue (Fig 3C,D, one-way ANOVA, F=20.48, p<0.0001,

Tukey's post-hoc test). These results suggest the involvement of S1166 in the GABAergic regulation of Ca2+ influx through NMDARs, though we cannot rule out the participation of other PKA targets.

To confirm that functional GluN2B subunits contribute to 2PLU-evoked NMDAR responses in our recordings, we measured NMDAR activation in the presence of the specific GluN2B antagonist ifenprodil (3 μM). Ifenprodil significantly reduced NMDAR currents (22.7 ± 1.8 pA, n=46 spines vs. 14.0 ± 1.4 pA, n=33 spines, p=0.0006, Fig S2C, D) and ΔCa2+ (0.54 ± 0.02 $\Delta G/G_{sat}$, n=46 spines vs. 0.44 ± 0.02 $\Delta G/G_{sat}$, n=33 spines, p=0.0003, Fig. S2). Thus, baclofen but not guanfacine diminishes synaptic Ca2+ influx through NMDARs via the dephosphorylation of the GluN2B subunit at the Serine 1166 residue. In summary, these results confirm that the surprisingly disparate actions of α2Rs and $GABA_BRs$ on glutamate receptors are all mediated by downregulation of PKA signaling.

Adrenergic and GABAergic actions are localized to the same dendritic spine

As our initial studies compared separate populations of spines in control and treatment conditions, one explanation for our findings is that either guanfacine or baclofen may act non-cell-autonomously such that the two PKA-dependent signaling pathways occur in different cells. To test this possibility, we co-applied guanfacine and baclofen while stimulating a single synapse using 2PLU. We monitored both uEPSCs and ΔCa2+ while voltage clamping the cell at either −70 mV or +40 mV to measure AMPAR- or NMDAR-mediated responses, respectively (Fig. 4). Compared to baseline, combined application of guanfacine and baclofen for 10 minutes decreased AMPAR currents (18.8 ± 2.8 pA vs. 12.1 ± 1.7 pA, n=6 spines, p=0.0163, paired t-test, Fig. 4A). As above, the drug combination did not change NMDAR-mediated currents (12.7 ± 2.5 pA vs. 15.6 ± 5.1 pA, n=6 spines, p=0.9220, paired t-test, Fig. 4B) but decreased ΔCa2+ (0.21 ± 0.04 $\Delta G/G_{sat}$ vs. 0.12 ± 0.03 $\Delta G/G_{sat}$, p= 0.0132, paired t-tests, Fig. 4C). Importantly, the combined actions of guanfacine and baclofen on AMPAR-mediated currents (n=6 spines, p=0.626, paired t-test) and NMDAR-mediated Ca2+ influx (n=6 spines, p=0.6555, paired t-test) were occluded by adding the membrane-impermeable PKA antagonist PKI(6-22) (20 μM) to the recording pipette (Fig. 4A-C). These results confirm that the PKA-dependent actions of α2Rs and $GABA_BRs$ cell-autonomously modulate both types of glutamate receptors.

Our results might also be explained if α2Rs and $GABA_BRs$ are not co-localized, giving rise to a physical segregation of signaling pathways that could produce a functional dissociation. To test this possibility, we performed three sets of experiments. First, we used a puffer pipette to locally apply a combination of guanfacine and baclofen to a small dendritic region while holding the cell at either −70 mV or +40 mV (Fig. 5A-D). This focal drug application yielded similar results to bath-application. AMPAR-mediated currents were decreased (19.7 ± 2.6 pA to 9.3 ± 1.9 pA, n=10, p=0.0083), NMDAR-mediated currents were not altered (11.4 ± 2.1 pA vs. 10.7 ± 2.1 pA, n=10, p=0.39), and NMDAR-mediated ΔCa2+ was decreased (0.22 ± 0.05 $\Delta G/G_{sat}$ vs. 0.088 ± 0.02 $\Delta G/G_{sat,}$ n=10, p=0.0055).

Second, we performed immunohistochemical triple-staining to test for co-localization of α2Rs and $GABA_BRs$ at the postsynaptic density (Fig. 5E,F, see Supplemental Methods).

α2Rs and $GABA_B$Rs were significantly more co-localized with the postsynaptic protein PSD95 than the presynaptic marker bassoon or a pixel-shuffled control.

Third, we tested the actions of α2Rs and $GABA_B$Rs on voltage-gated calcium channels (VGCCs), known to be modulated by a PKA-independent pathway involving the membrane delimited beta-gamma subunits (Gβγ) associated with $G\alpha_i$ (Yan and Surmeier, 1996, Herlitze et al., 1996). We monitored VGCC-dependent ΔCa2+ in spines and adjacent dendritic shafts evoked by back-propagating action potentials (bAPs, Fig. S3, see Methods) (Sabatini and Svoboda, 2000). Under control conditions, ΔCa2+ in spines was 0.052 ± 0.003 $\Delta G/G_{sat}$ (n=34 spines). In the presence of either guanfacine or baclofen, ΔCa2+ was 0.029 ± 0.002 $\Delta G/G_{sat}$ (n=38 spines) or 0.031 ± 0.001 $\Delta G/G_{sat}$ (n=41 spines), respectively. Combined application of guanfacine and baclofen produced a ΔCa2+ of 0.036 ± 0.003 $\Delta G/G_{sat}$ (n=33 spines, Fig. S3B-E). One-way ANOVA ($F=20.52$, $p<0.0001$) with post-hoc testing revealed that both guanfacine and baclofen significantly reduced ΔCa2+, but there was no additional effect of combining the two drugs. Similar results were seen for ΔCa2+ in the corresponding dendritic shafts. These results indicate modulation of physically overlapping pools of VGCCs. Thus, the combination of findings strongly supports the conclusion that α2Rs and $GABA_B$Rs are co-localized in the same dendritic spines.

Preferential structural co-localization of GPCRs with glutamate receptors

Our results indicate functional coupling of α2Rs with AMPARs and $GABA_B$Rs with NMDARs. To determine whether these receptor groupings have a structural underpinning, we performed a proximity ligation assay that identifies proteins localized within 10-15 nm from each other (Soderberg et al., 2006). Co-staining for GluA1 and α2R produced significantly higher labeling density than for GluA1 and $GABA_B$R (1.7 ± 0.2 vs. 0.9 ± 0.1 puncta per 100 μm^2, n=31 images from 3 mice, p=0.0004). Similarly, co-staining for NR1 and $GABA_B$R produced significantly higher labeling density than for NR1 and α2R (1.2 ± 0.09 vs 0.76 ± 0.08 puncta per 100 μm^2, n=31 images from 3 mice, p=0.0004, Fig. 6). This preferential structural localization of α2Rs/AMPARs and $GABA_B$Rs/NMDARs at synapses suggests the existence of synaptic microdomains where neuromodulation can occur independently despite utilization of similar biochemical signaling pathways.

RGS4 limits the crosstalk between different $G\alpha_i$ coupled receptors

Our results suggest the surprising conclusion that separate, parallel modulation of glutamate receptors occurs without biochemical crosstalk in single spines. Notably, although activation of $G_{i/o}$-coupled receptors decreases the amount of cAMP and active PKA in the spine, the concentration of the active mobile $G\alpha_i$ subunit is increased. Thus, some mechanism must limit the functional mobility of $G\alpha_i$ to prevent signaling crosstalk. One such mechanism might involve Regulators of G-protein Signaling (RGS) proteins that accelerate hydrolysis of GTP to GDP, hastening the self-inactivation of $G\alpha_i$ (Arshavsky and Pugh, 1998, Watson et al., 1996, Zhong et al., 2003). To test this possibility, we measured 2PLU-evoked synaptic currents and corresponding Ca2+ transients in the presence of a selective small molecule inhibitor (CCG50014, (Blazer et al., 2011, Turner et al., 2012)) that targets RGS4, the most abundant RGS family member in layer 5 pyramidal neurons of the PFC (Ebert et al., 2006, Gold et al., 1997).

CCG50014 (5 μM) by itself did not alter responses mediated by either NMDARs or AMPARs (Fig. 7A-C). However, in contrast to our earlier findings, in the presence of CCG50014, baclofen produced a significant reduction in AMPAR-mediated currents (17.5 ± 1.6 pA, n=31 spines vs. 10.0 ± 1.1 pA, n=32 spines, p<0.001). Guanfacine also reduced AMPAR-mediated currents (to 9.7 ± 0.8 pA, n=30 spines, p<0.001) similarly to guanfacine alone (p>0.05)(Fig. 7A). Conversely, in the presence of CCG50014, guanfacine produced a significant reduction in NMDAR-mediated currents (27.6 ± 2.8 pA, n=30 spines vs. 15.4 ± 2.4, n=32 spines, p<0.01) and ΔCa2+ (0.68 ± 0.03 $\Delta G/G_{sat}$ vs. 0.5 ± 0.03 $\Delta G/G_{sat}$, p<0.001, Fig. 7B, C). Notably, in combination with CCG50014, baclofen also reduced NMDAR-mediated currents (to 7.8 ± 1.2 pA, n=35 spines, p<0.001, Fig 7A and C) and ΔCa2+ (to 0.37 ± 0.03 $\Delta G/G_{sat}$ in CCG50014+baclofen, p<0.001, Fig B, C).

To confirm the specificity of our results, we dialyzed neurons with an antibody against RGS4 via the patch pipette, a method previously shown to specifically inhibit RGS4 function (Liu et al., 2006), and performed similar experiments (Fig. S4). We found that, with the RGS4 antibody in the pipette solution, baclofen significantly reduced AMPAR-mediated currents (21.1 ± 1.6 pA, n=30 spines vs. 14.14 ± 0.98 pA, n=32 spines, p=0.0003). In complementary experiments, in the presence of the RGS4 antibody, guanfacine reduced NMDAR-mediated currents (20.7 ± 2 pA n=31 spines vs. 7.15 ± 1.3 pA, n=34 spines, p<0.0001) and ΔCa2+ (0.633 ± 0.017 $\Delta G/G_{sat}$ vs. 0.34 ± 0.02 $\Delta G/G_{sat}$, p<0.0001). In conclusion, our data indicate that RGS4 prevents cross-talk between biochemical signaling cascades and preserves neuromodulatory specificity.

Discussion

Multiple neuromodulatory systems coupled to GPCRs share common signal transduction pathways. In the prefrontal cortex, neuronal activity is regulated by $G\alpha_i$-mediated signaling through receptors for norepinephrine, GABA, dopamine (D2), and acetylcholine (M2,M4). However, it remains largely unknown how individual neurons distinguish between these modulatory inputs and prevent crosstalk between similar biochemical signaling pathways. Here, we found that activation of α2Rs and $GABA_BRs$ selectively inhibits AMPARs and NMDARs, respectively, and that this modulation occurs at single glutamatergic synapses. In both cases, the regulation of glutamate receptors occurs via a $G\alpha_i$-dependent reduction in PKA activity. Our evidence suggests that all four receptors are present in individual spines with a preferential co-localization (< 20 nm) of α2Rs/AMPARs and $GABA_BRs$/NMDARs. Under control conditions, cross-talk between α2R- and $GABA_BR$-coupled signaling cascades is prevented by the actions of RGS4, a GTPase Activating Protein (GAP) that targets $G\alpha_i$ (Watson et al., 1996). Our results provide evidence for a mechanism by which biochemical signaling pathways are functionally compartmentalized and highlight the role of RGS4 in regulating synaptic transmission (Fig. S5). In future studies, it will be interesting to determine whether other modulatory pathways (e.g., D2 dopamine receptors) obey similar compartmentalization to regulate specific glutamate receptors.

Establishment of synaptic microdomains for neuromodulation

Our data show that, under control conditions, there is no cross-talk between α2R- and $GABA_BR$-mediated modulation of glutamate receptors despite similar actions on cAMP and PKA activity. One explanation for this compartmentalization is that α2Rs and $GABA_BRs$ are located on different dendritic spines. We excluded this possibility by (1) showing that AMPAR- and NMDAR-dependent synaptic responses evoked by stimulation of a single spine are reduced by focal co-application of guanfacine and baclofen, (2) showing that α2Rs and $GABA_BRs$ co-localize with PSD95, and (3) finding that guanfacine and baclofen mutually occlude each other's modulation of VGCCs. A second explanation for our data is that one or both of the actions of guanfacine and baclofen occur via distinct, non-cell-autonomous mechanisms. However, we find that loading single cells with a membrane impermeable PKA antagonist occludes the modulation of both AMPARs and NMDARs, arguing that the relevant α2Rs and $GABA_BRs$ are localized to the recorded neuron.

A third possibility is that α2Rs and $GABA_BRs$ are located in the same spines, and the lack of cross-talk is mediated by functional compartmentalization of signaling cascades. This latter conclusion is strongly supported by our results, which suggest a functional microdomain established by the limited lifetime of $G\alpha_i$, whose signaling is terminated by its endogenous GTPase activity (Arshavsky and Pugh, 1998). The ability of $G\alpha_i$ subunits to hydrolyze GTP is strongly accelerated by Regulators of G-protein Signaling (RGS) proteins (Watson et al., 1996). Of this protein family, RGS4 is strongly expressed in layer 5 of the PFC (Ebert et al., 2006). Here, we show that blocking RGS4 activity pharmacologically (CCG50014) or by dialyzing the cells with an antibody against RGS4, impairs the selectivity of $G\alpha_i$-coupled neuromodulators, thus enabling cross-talk of second messenger systems and leading to a breakdown in signal specificity in dendritic spines of layer 5 pyramidal neurons (Fig. S5). Notably, previous computational work explicitly predicted a role for RGS4 in restricting $G\alpha_i$ signaling to a small microdomain (Zhong et al., 2003). In this model, high RGS4 activity can limit diffusion of GTP-bound $G\alpha_i$ to < 20 nm. This suggestion is supported by our proximity ligation assay data, which suggest preferential postsynaptic coupling of α2Rs/AMPARs and $GABA_BRs$/NMDARs within 20 nm (Soderberg et al., 2006). There is mounting anatomical evidence that synaptic proteins, including glutamate receptors, are organized into 70-80 nm clusters within the postsynaptic density (MacGillavry et al., 2013, Nair et al., 2013). Precedent for such structural links was shown previously for a presynaptic β2-adrenergic-AMPAR signaling complex allowing highly localized cAMP signaling in the hippocampus (Joiner et al., 2010). Here, we demonstrate a functional role for these nano-structures and provide a plausible biochemical mechanism for the segregation of signaling domains within a single synapse.

We note that an additional explanation for our results is that both adrenergic and GABAergic activity stimulates an unidentified non-canonical (e.g., not adenylate cyclase-mediated) signaling pathway that inhibits cross-modulation of glutamate receptors. While possible, this explanation seems unlikely given the findings that two independent methods of blocking RGS4 activity lead to cross-modulation. Thus, this alternative explanation would require the existence of an unidentified GPCR-coupled pathway that is also regulated by RGS4.

Surprisingly, we find that blocking RGS4 activity allows both guanfacine and baclofen to modulate the total current through NMDARs in addition to the Ca2+ influx. A similar result was seen when blocking PKA signaling directly with H89. This result suggests a second PKA target on the NMDAR, in addition to GluN2B S1166, such as GluN1 S897, that controls total current magnitude. We propose that modest reduction in PKA signaling (as occurs with activation of $GABA_BRs$) influences Ca2+ influx by selectively dephosphorylating S1166, while stronger reduction in PKA signaling (either with a pharmacological block or the increased activity of $G\alpha_i$ following RGS4 block) leads to decreased Ca2+ and total current by dephosphorylating multiple targets.

Functionally, our findings suggest that distinct modulatory systems coupled to PKA signaling differentially impact synaptic integration. Specifically, adrenergic actions via α2Rs are expected to reduce electrical summation of inputs leading to a reduction in neuronal output. In contrast, GABAergic actions are expected to regulate summation of local dendritic Ca2+ signals, potentially influencing synaptic plasticity. Thus, breakdown in the functional segregation of these pathways might lead to aberrant modulation and dysregulation of cellular activity. Indeed, mutations in RGS4 have been linked to neuropsychiatric disorders such as schizophrenia (Levitt et al., 2006). Future studies are necessary to investigate the interactions of RGS4 and neuromodulatory signaling in disease.

Experimental procedures

Slice Preparation

All animal handling was performed in accordance with guidelines approved by the Yale Institutional Animal Care and Use Committee and federal guidelines. Acute prefrontal cortical (PFC) slices (300 μm) were prepared from wild-type C57/Bl6 mice (P22-36) and maintained in artificial cerebrospinal fluid (ACSF) containing (in mM): 126 NaCl, 26 $NaHCO_3$, 1.25 NaH_2PO_4, 3 KCl, 1 $MgCl_2$, 2 $CaCl_2$, 10 glucose, 0.4 sodium ascorbate, 2 sodium pyruvate and 3 myo-inositol, bubbled with 95% O_2 and 5% CO_2.

Electrophysiology and imaging

All experiments were conducted at near physiological temperature (32-34°C). For voltage-clamp recordings, glass electrodes (1.8-3.0 MΩ) were filled with internal solution containing (in mM): 135 $CsMeSO_3$, 10 HEPES, 4 $MgCl_2$, 4 Na_2ATP, 0.4 NaGTP, 10 sodium creatine phosphate and 0.2% Neurobiotin (Vector Laboratories), Alexa Fluor-594 (10 μM), Fluo-5F (300 μM), adjusted to pH 7.3 with CsOH. Electrophysiological recordings were made using a Multiclamp 700B amplifier, filtered at 4 kHz, and digitized at 10 kHz.

2-photon imaging was accomplished with a custom-modified Olympus BX51-WI microscope. Fluorophores were excited using 840 nm light from a pulsed titanium-sapphire laser and emissions collected by photomultiplier tubes (Hamamatsu).

For focal stimulation of single dendritic spines, we used 2-photon laser uncaging of glutamate (2PLU). To photorelease glutamate, a second Ti-Sapphire laser tuned to 720 nm was introduced into the light path using polarization optics. Back propagating action

potentials (bAPs) were evoked by injecting brief current pulses (2 nA, 2 ms) into the cell through the recording pipette.

Data acquisition and analysis

Imaging and physiology data were acquired using National Instruments data acquisition boards and custom software written in MATLAB. Off-line analysis was performed using custom routines written in MATLAB and IgorPro. Statistical comparisons were conducted in GraphPad Prism 5. Unless otherwise stated, all data were analyzed using two-tailed, unpaired T-tests.

Pharmacology and reagents

2PLU experiments were performed in normal ACSF supplemented with MNI-glutamate (2.5 mM) and D-serine (10 μM). To isolate AMPAR-mediated currents, we added TTX (1 μM), picrotoxin (50 μM), CGP55845 (3 μM), and CPP (10 μM) to the ACSF. To isolate NMDAR-mediated currents, we modified our original ACSF to contain 0 mM Mg and 3 mM Ca^{2+} and included TTX (1 μM), picrotoxin (50 μM), CGP55845 (3 μM), and NBQX 10 μM. In experiments investigating the effects of baclofen, CGP55845 was omitted from the solutions. For PKA pharmacology, we applied H89 (10 μM) or N6-benzo-cAMP (100 μM, Millipore). In some experiments, we included PKI(6-22) (20 μM) in the recording pipette. To block the actions of RGS4 we added CCG50014 (5 μM). All compounds were from Tocris except where noted.

Western blot analysis

Brain slices containing the PFC were prepared as described and incubated with normal ACSF for control or ACSF supplemented with either guanfacine 40 μM, baclofen 5 μM, H89 10 μM or forskolin 50 μM for 10 minutes at 32-34°C before the prefrontal cortex was dissected out, homogenised and lysed in 20 mM Tris, 1 mM EDTA and 1x Halt protease and phosphatase inhibitor cocktail and 0.5% SDS, pH 8.0. After centrifugation samples were separated by SDS-PAGE and transferred to PVDF membranes. Primary antibodies against phosphorylated GluA1 S845, phosphorylated GluN2B S1166 or RGS4 were applied overnight. Bands were visualized using standard HRP procedures. Membranes were then stripped from antibodies, re-blocked and immunoreacted with non-phospho specific anti-GluA1, anti-GluN2B or anti-β-tubulin primary antibody to establish total amount of GluA1, GluN2B or β-tubulin in the samples. Scanned autoradiography images were analyzed with ImageJ. Phosphorylation was quantified as phoshorylated / total protein and normalized to the control values of each experiment.

Immunofluorescence and proximity ligation assay (PLA)

C57/bl6 mice were transcardially perfused with phosphate buffer (PB) followed by 4% paraformaldehyde. To expose synaptic proteins, sections (70 μm) containing the PFC were permeabilised with 0.1% Triton X-100 then treated with 0.25 mg/ml pepsin for 10 minutes at 37 °C in 0.2 N HCl. Primary antibodies against PSD95 or Bassoon, α2R and $GABA_bR$ were applied overnight. Following secondary antibody staining images were collected from

the PFC region and analysed in Cell Profiler. Co-localization is given as the percentage of PSD95 or Bassoon puncta overlapping with both α2R and $GABA_BR$ staining.

To perform proximity ligation assay, 70 μm sections containing the PFC were obtained from 3 mice and pepsin treated as described. Glutamate receptors were co-labelled with GPCRs using primary antibodies against GluA1 or GluN1 and α2R or $GABA_bR$. PLA was performed using a Duolink In Situ kit (SIGMA) in accordance with the manufacturer's instructions. Images were randomly collected from the PFC region of the sections and analyzed in Cell Profiler.

Supplementary Material

Refer to Web version on PubMed Central for supplementary material.

Acknowledgements

The authors thank J. Cardin, S. Tomita, and members of the Higley laboratory for comments during the preparation of this manuscript. The work was funded by grants from the Smith Family Foundation (M.J.H.), The Yale Brown-Coxe Memorial Fund (G.L.), The Brain and Behavior Research Foundation (M.J.H. and G.L.), and the NIH: MH099045 (M.J.H.).

References

ARNSTEN AF. Catecholamine influences on dorsolateral prefrontal cortical networks. Biol Psychiatry. 2011; 69:e89–99. [PubMed: 21489408]

ARSHAVSKY VY, PUGH EN JR. Lifetime regulation of G protein-effector complex: emerging importance of RGS proteins. Neuron. 1998; 20:11–4. [PubMed: 9459437]

BLAZER LL, ZHANG H, CASEY EM, HUSBANDS SM, NEUBIG RR. A nanomolar-potency small molecule inhibitor of regulator of G-protein signaling proteins. Biochemistry. 2011; 50:3181–92. [PubMed: 21329361]

CARTER AG, SABATINI BL. State-dependent calcium signaling in dendritic spines of striatal medium spiny neurons. Neuron. 2004; 44:483–93. [PubMed: 15504328]

CHALIFOUX JR, CARTER AG. GABAB receptors modulate NMDA receptor calcium signals in dendritic spines. Neuron. 2010; 66:101–13. [PubMed: 20399732]

CHEN G, CHEN P, TAN H, MA D, DOU F, FENG J, YAN Z. Regulation of the NMDA receptor-mediated synaptic response by acetylcholinesterase inhibitors and its impairment in an animal model of Alzheimer's disease. Neurobiol Aging. 2008; 29:1795–804. [PubMed: 17555845]

DESTEXHE A, MAINEN ZF, SEJNOWSKI TJ. Synthesis of models for excitable membranes, synaptic transmission and neuromodulation using a common kinetic formalism. J Comput Neurosci. 1994; 1:195–230. [PubMed: 8792231]

DISMUKES RK. New Concepts of Molecular Communication among Neurons. Behavioral and Brain Sciences. 1979; 2:409–416.

EBERT PJ, CAMPBELL DB, LEVITT P. Bacterial artificial chromosome transgenic analysis of dynamic expression patterns of regulator of G-protein signaling 4 during development. I. Cerebral cortex. Neuroscience. 2006; 142:1145–61. [PubMed: 16996696]

ESTEBAN JA, SHI SH, WILSON C, NURIYA M, HUGANIR RL, MALINOW R. PKA phosphorylation of AMPA receptor subunits controls synaptic trafficking underlying plasticity. Nat Neurosci. 2003; 6:136–43. [PubMed: 12536214]

GAMO NJ, ARNSTEN AF. Molecular modulation of prefrontal cortex: rational development of treatments for psychiatric disorders. Behav Neurosci. 2011; 125:282–96. [PubMed: 21480691]

GOLD SJ, NI YG, DOHLMAN HG, NESTLER EJ. Regulators of G-protein signaling (RGS) proteins: region-specific expression of nine subtypes in rat brain. J Neurosci. 1997; 17:8024–37. [PubMed: 9315921]

HERLITZE S, GARCIA DE, MACKIE K, HILLE B, SCHEUER T, CATTERALL WA. Modulation of Ca2+ channels by G-protein beta gamma subunits. Nature. 1996; 380:258–62. [PubMed: 8637576]

HIGLEY MJ, SABATINI BL. Calcium signaling in dendrites and spines: practical and functional considerations. Neuron. 2008; 59:902–13. [PubMed: 18817730]

JI XH, JI JZ, ZHANG H, LI BM. Stimulation of alpha2-adrenoceptors suppresses excitatory synaptic transmission in the medial prefrontal cortex of rat. Neuropsychopharmacology. 2008; 33:2263–71. [PubMed: 17957212]

JOINER ML, LISE MF, YUEN EY, KAM AY, ZHANG M, HALL DD, MALIK ZA, QIAN H, CHEN Y, ULRICH JD, BURETTE AC, WEINBERG RJ, LAW PY, EL-HUSSEINI A, YAN Z, HELL JW. Assembly of a beta2-adrenergic receptor--GluR1 signalling complex for localized cAMP signalling. EMBO J. 2010; 29:482–95. [PubMed: 19942860]

KESNER RP, CHURCHWELL JC. An analysis of rat prefrontal cortex in mediating executive function. Neurobiol Learn Mem. 2011; 96:417–31. [PubMed: 21855643]

KNIGHT AR, BOWERY NG. The pharmacology of adenylyl cyclase modulation by GABAB receptors in rat brain slices. Neuropharmacology. 1996; 35:703–12. [PubMed: 8887979]

KULIK A, VIDA I, LUJAN R, HAAS CA, LOPEZ-BENDITO G, SHIGEMOTO R, FROTSCHER M. Subcellular localization of metabotropic GABA(B) receptor subunits GABA(B1a/b) and GABA(B2) in the rat hippocampus. J Neurosci. 2003; 23:11026–35. [PubMed: 14657159]

LEVITT P, EBERT P, MIRNICS K, NIMGAONKAR VL, LEWIS DA. Making the case for a candidate vulnerability gene in schizophrenia: Convergent evidence for regulator of G-protein signaling 4 (RGS4). Biol Psychiatry. 2006; 60:534–7. [PubMed: 16860780]

LISMAN JE, RAGHAVACHARI S, TSIEN RW. The sequence of events that underlie quantal transmission at central glutamatergic synapses. Nat Rev Neurosci. 2007; 8:597–609. [PubMed: 17637801]

LIU W, YUEN EY, ALLEN PB, FENG J, GREENGARD P, YAN Z. Adrenergic modulation of NMDA receptors in prefrontal cortex is differentially regulated by RGS proteins and spinophilin. Proc Natl Acad Sci U S A. 2006; 103:18338–43. [PubMed: 17101972]

MACGILLAVRY HD, SONG Y, RAGHAVACHARI S, BLANPIED TA. Nanoscale scaffolding domains within the postsynaptic density concentrate synaptic AMPA receptors. Neuron. 2013; 78:615–22. [PubMed: 23719161]

MURPHY JA, STEIN IS, LAU CG, PEIXOTO RT, AMAN TK, KANEKO N, AROMOLARAN K, SAULNIER JL, POPESCU GK, SABATINI BL, HELL JW, ZUKIN RS. Phosphorylation of Ser1166 on GluN2B by PKA is critical to synaptic NMDA receptor function and Ca2+ signaling in spines. J Neurosci. 2014; 34:869–79. [PubMed: 24431445]

NAIR D, HOSY E, PETERSEN JD, CONSTALS A, GIANNONE G, CHOQUET D, SIBARITA JB. Super-resolution imaging reveals that AMPA receptors inside synapses are dynamically organized in nanodomains regulated by PSD95. J Neurosci. 2013; 33:13204–24. [PubMed: 23926273]

RAYMOND LA, TINGLEY WG, BLACKSTONE CD, ROCHE KW, HUGANIR RL. Glutamate receptor modulation by protein phosphorylation. J Physiol Paris. 1994; 88:181–92. [PubMed: 7530547]

SABATINI BL, SVOBODA K. Analysis of calcium channels in single spines using optical fluctuation analysis. Nature. 2000; 408:589–93. [PubMed: 11117746]

SODERBERG O, GULLBERG M, JARVIUS M, RIDDERSTRALE K, LEUCHOWIUS KJ, JARVIUS J, WESTER K, HYDBRING P, BAHRAM F, LARSSON LG, LANDEGREN U. Direct observation of individual endogenous protein complexes in situ by proximity ligation. Nat Methods. 2006; 3:995–1000. [PubMed: 17072308]

STAN AD, LEWIS DA. Altered cortical GABA neurotransmission in schizophrenia: insights into novel therapeutic strategies. Curr Pharm Biotechnol. 2012; 13:1557–62. [PubMed: 22283765]

SUMMERS RJ, MCMARTIN LR. Adrenoceptors and their second messenger systems. J Neurochem. 1993; 60:10–23. [PubMed: 8380191]

TURNER EM, BLAZER LL, NEUBIG RR, HUSBANDS SM. Small Molecule Inhibitors of Regulator of G Protein Signalling (RGS) Proteins. ACS Med Chem Lett. 2012; 3:146–150. [PubMed: 22368763]

TYACKE RJ, LINGFORD-HUGHES A, REED LJ, NUTT DJ. GABAB receptors in addiction and its treatment. Adv Pharmacol. 2010; 58:373–96. [PubMed: 20655489]

WANG M, RAMOS BP, PASPALAS CD, SHU Y, SIMEN A, DUQUE A, VIJAYRAGHAVAN S, BRENNAN A, DUDLEY A, NOU E, MAZER JA, MCCORMICK DA, ARNSTEN AF. Alpha2A-adrenoceptors strengthen working memory networks by inhibiting cAMP-HCN channel signaling in prefrontal cortex. Cell. 2007; 129:397–410. [PubMed: 17448997]

WATSON N, LINDER ME, DRUEY KM, KEHRL JH, BLUMER KJ. RGS family members: GTPase-activating proteins for heterotrimeric G-protein alpha-subunits. Nature. 1996; 383:172–5. [PubMed: 8774882]

YAN Z, SURMEIER DJ. Muscarinic (m2/m4) receptors reduce N- and P-type Ca2+ currents in rat neostriatal cholinergic interneurons through a fast, membrane-delimited, G-protein pathway. J Neurosci. 1996; 16:2592–604. [PubMed: 8786435]

YUSTE R, MAJEWSKA A, HOLTHOFF K. From form to function: calcium compartmentalization in dendritic spines. Nat Neurosci. 2000; 3:653–9. [PubMed: 10862697]

ZHONG H, WADE SM, WOOLF PJ, LINDERMAN JJ, TRAYNOR JR, NEUBIG RR. A spatial focusing model for G protein signals. Regulator of G protein signaling (RGS) protien-mediated kinetic scaffolding. J Biol Chem. 2003; 278:7278–84. [PubMed: 12446706]

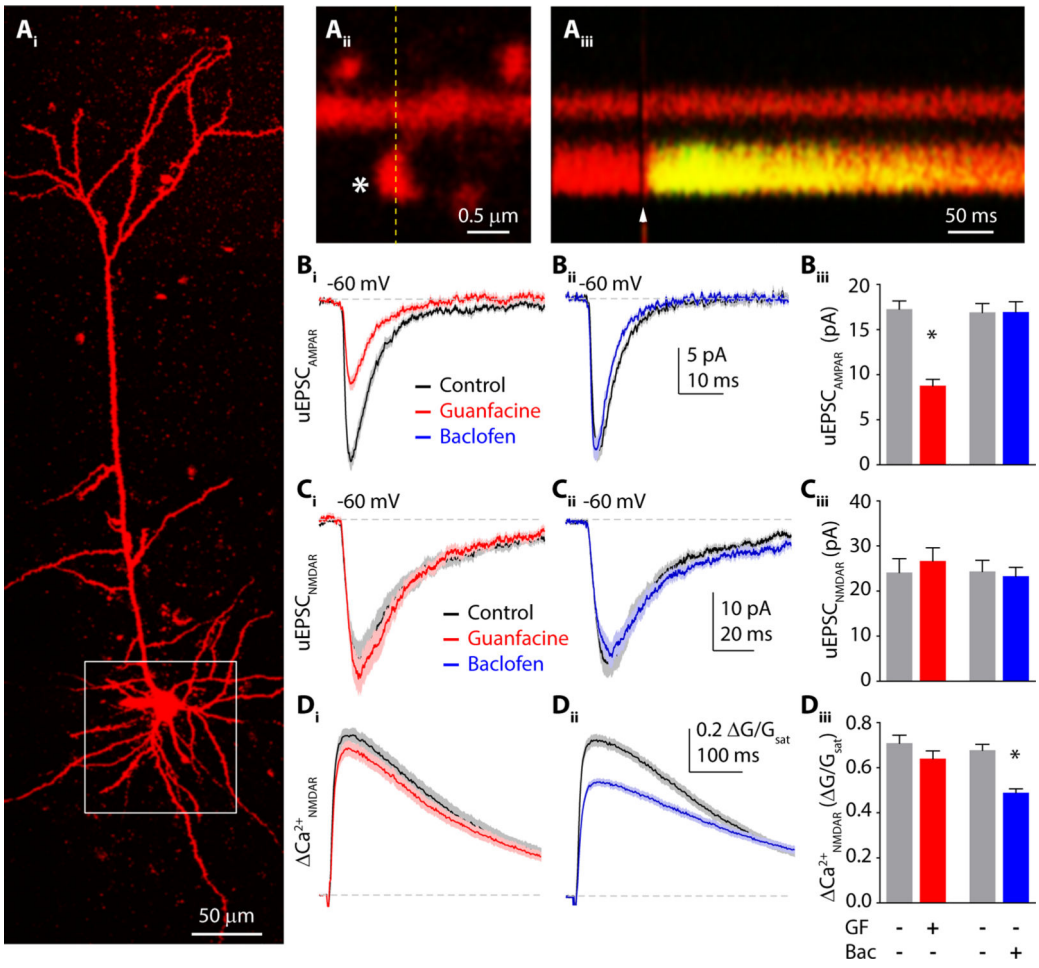

Figure 1.

α2Rs and $GABA_BRs$ differentially modulate AMPA- and NMDA-type glutamate receptors. (**Ai**) 2-photon image of a layer 5 pyramidal neuron filled with Alexa Fluor 594 dye via the patch pipette. White box indicates the basal dendritic arbor. (**Aii**) Close up image of a dendritic spine. Asterisk shows the location of glutamate uncaging. (**Aiii**) Fluorescence collected in a line scan indicated on (**Aii**) by dashed line. Arrowhead shows the time point of glutamate uncaging. (**Bi**) Mean AMPAR mediated uEPSCs in control (black) and guanfacine (red) ± SEM (shaded areas). (**Bii**) AMPAR mediated uEPSCs in control (black) and baclofen (blue) ± SEM (shaded areas). (**Biii**) Bars represent mean uEPSC amplitudes in control (gray), guanfacine (red) and baclofen (blue) ± SEM. (**Ci**) 2PLU-evoked NMDAR-currents and (**Di**) Ca2+ transients in control (black) and guanfacine (red), mean (solid lines) ± SEM (shaded areas). (**Cii**) NMDAR-mediated uEPSCs and (**Dii**) Ca2+ transients in control (black) and baclofen (blue) ± SEM (shaded areas). (**Ciii**) Bars represent mean uEPSC amplitudes in control (gray), guanfacine (red) and baclofen (blue) ± SEM. (**Diii**) Mean amplitude of NMDAR Ca2+ transients in control (gray), guanfacine (red) and baclofen (blue) ± SEM. *: $p<0.05$, unpaired t-test.

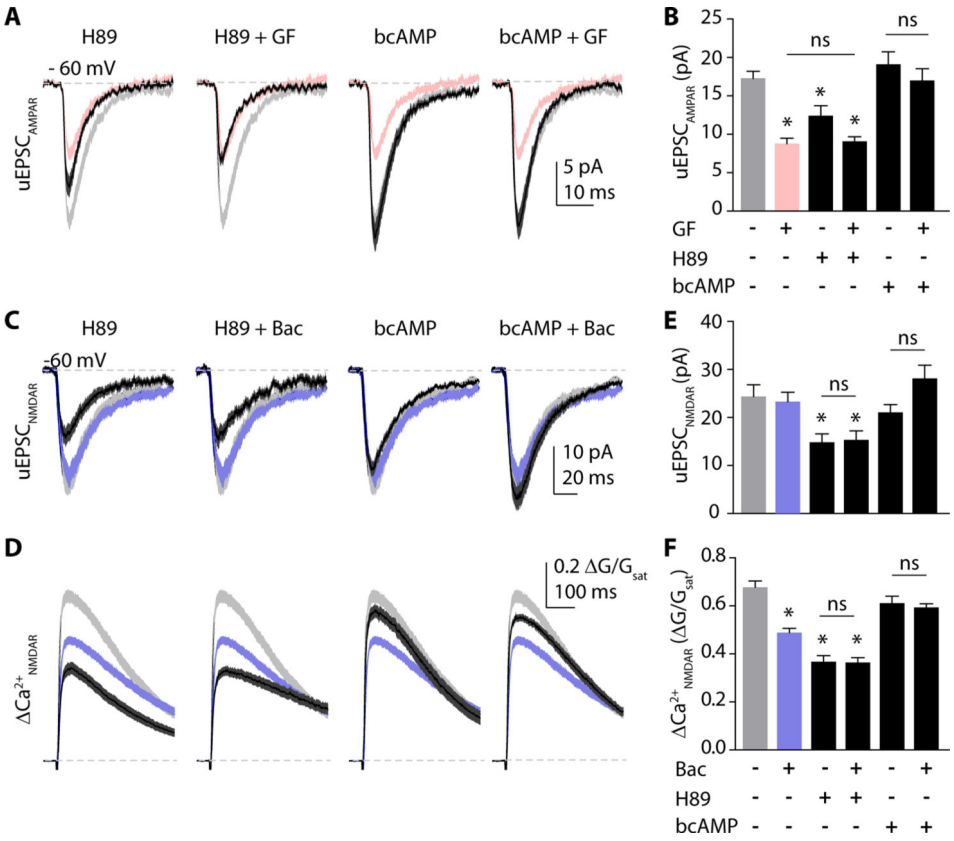

Figure 2.

Both α2R modulation of AMPARs and $GABA_BR$ modulation of NMDARs are mediated by downregulation of PKA. (**A**) AMPAR-mediated uEPSCs. Solid black lines show mean ± SEM (dark gray shading) for responses in the PKA antagonist H89 (10 μM), H89 + guanfacine (40 μM), the PKA activator N-6-benzo-cAMP (bcAMP, 100 μM), or bcAMP + guanfacine (left to right). Light gray and red shaded areas represent mean ± SEM of control and guanfacine groups, respectively, for comparison. (**B**) Bars represent mean amplitudes ± SEM of uEPSC under the above conditions. (**C**) NMDAR-mediated uEPSCs. Solid black lines show mean ± SEM (dark gray shading) for responses in the PKA antagonist H89 (10 μM), H89 + baclofen (5 μM),the PKA activator bcAMP (100 μM), or bcAMP + baclofen (left to right). Light gray and blue shaded areas represent mean ± SEM of control and baclofen groups, respectively, for comparison. (**D**) 2PLU-evoked Ca2+ transients under the same conditions as in (**C**). (**E**) Bars represent mean amplitudes ± SEM of uEPSC and (**F**) Ca2+ transients under the above conditions. *: $p<0.05$, Tukey`s multiple comparison test.

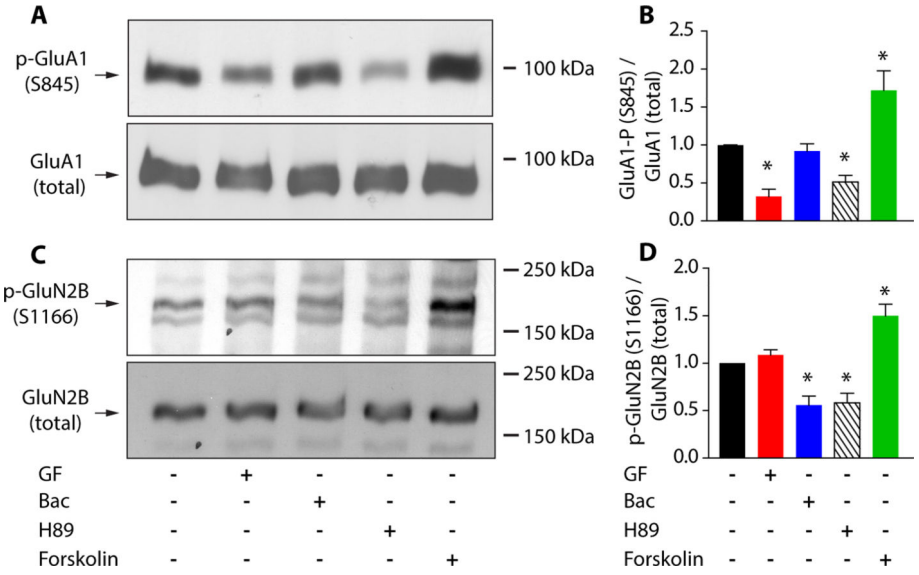

Figure 3.

α2R and $GABA_BR$ activation reduces GluA1 (S845) and GluN2B (S1166) phosphorylation in the PFC, respectively. (**A**) Western blot for phosphorylated GluA1 (S845) in prefrontal tissue lysates, left to right: under control (n=6 animals), guanfacine (40 μM, n=5 animals), baclofen (5 μM, n=5 animals), H89 (10 μM, n=5 animals) or forskolin (50 μM, n=4 animals) conditions (top). Membranes were then re-blotted for total GluA1 (bottom). (**B**) Quantification of S845 phosphorylation. Bars show mean ± SEM normalized to control (black) in guanfacine (red), baclofen (blue) and H89 (striped) and forskolin (green). (**C**) Western blots depicting GluN2B (S1166) phosphorylation (top) and total GluN2B (bottom) in, left to right: control (n=5 animals), guanfacine (40 μM, n=6 animals), baclofen (5 μM, n=6 animals), H89 (10 μM, n=5 animals) or forskolin (50 μM, n=5 animals). (**D**) Bars represent mean ± SEM S1166 phosphorylation in control (black), guanfacine (red), baclofen (blue), H89 (striped) and forskolin (green). *: $p<0.05$, Tukey`s multiple comparison test.

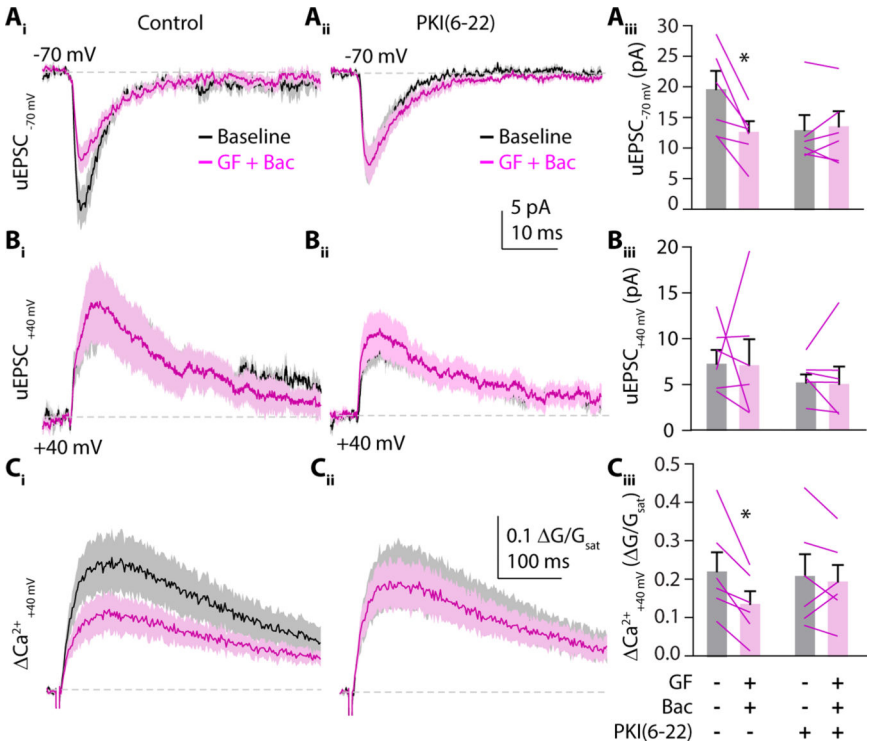

Figure 4.

α2Rs and $GABA_B$Rs cell autonomously modulate glutamate receptors. (**Ai**) Mean ± SEM traces (solid lines and shaded areas, respectively) of 2PLU-evoked uEPSCs from a single spine with the cell voltage clamped at −70 mV or at (**Bi**) +40 mV to measure AMPAR- and NMDAR-mediated currents, respectively. Black traces are uEPSCs during baseline recording, magenta traces show currents following 10 minutes exposure to guanfacine plus baclofen (n=6 spines on 6 cells). (**Ci**) Mean ± SEM traces (solid lines and shaded areas, respectively) showing ΔCa2+ traces with the cell voltage clamped at +40mV during baseline (black) and after guanfacine plus baclofen flow in (magenta) (**Aii-Cii**) Same experiment as in (**Ai-Ci**) but with the membrane-impermeable PKA inhibitor PKI(6-22) (20μM) in the recording pipette (n=6 spines on 6 cells). (**Aiii**, **Biii**) Mean ± SEM uEPSC amplitudes (bars) and for each individual cell (lines) recorded at −70 or +40 mV holding potential during baseline (gray) and post guanfacine and baclofen (magenta) using control- or PKI(6-22)-containing pipette solution. (**Ciii**) As above for NMDAR-mediated Ca2+ transients. *: $p<0.05$, paired t-test.

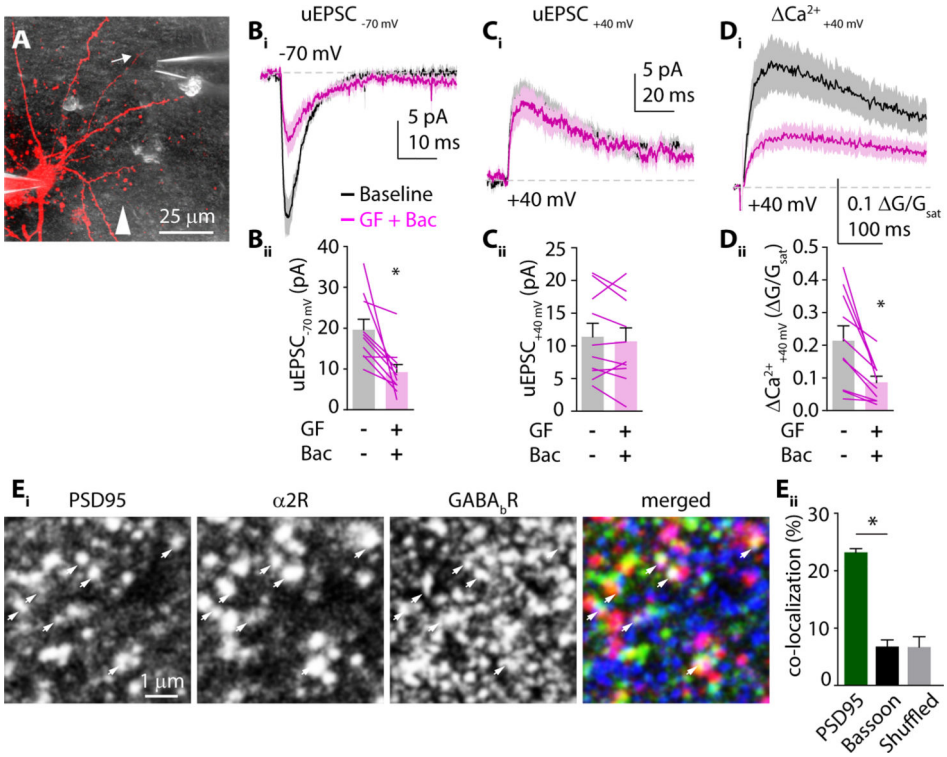

Figure 5.

α2Rs and $GABA_B$Rs are in the same dendritic spine. (**A**) 2-photon image of a L5 pyramidal neuron (red) and 2-photon DIC image (gray) showing the puffer pipette near the recorded denritic spine (arrow). White arrowhead is pointing in the direction of ACSF flow in the chamber. (**Bi**) Mean ± SEM uEPSC traces (solid lines and shaded areas, respectively) of 2PLU-evoked uEPSCs from a single spine with the cell voltage clamped at −70 mV or at (**Ci** and **Di**) +40 mV to measure AMPAR- and NMDAR-mediated currents and Ca2+ influx, respectively. Black traces are uEPSCs during baseline recording, magenta traces show currents following 10 minutes exposure to locally applied guanfacine plus baclofen (n=10 spines on 10 cells). (**Aii-Cii**) uEPSC and Ca2+ transient amplitudes: mean ± SEM (bars) and for each individual cell separately (lines) recorded at −70 or +40 mV holding potential during baseline (gray) and post guanfacine and baclofen (magenta). (**Ei**) Representative confocal images of PSD95 (green), α2R (red) and $GABA_B$R (blue) co-staining. White arrows point to both GPCRs co-localizing with PSD95. (**Eii**) Bars showing average co-localization of both α2Rs and $GABA_B$Rs with PSD95 (green) or Bassoon (black) in original or pixel-shifted (gray) images.

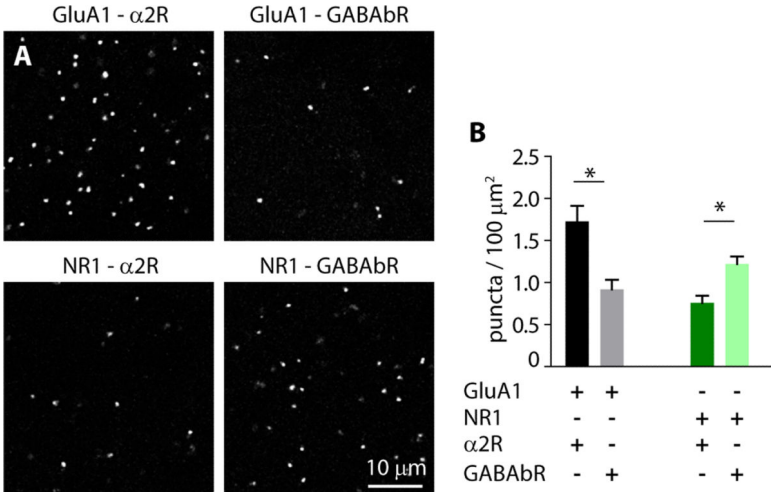

Figure 6.

α2Rs preferentially localize near AMPARs while $GABA_BRs$ preferentially localize near NMDARs. (**A**) Representative confocal images from PFC sections after proximity ligation assay. Tissue was stained with antibodies against the indicated targets. Bright puncta indicate positive PLA reactions. (**B**) Bars indicate mean ± SEM number of puncta per 100 μm2.

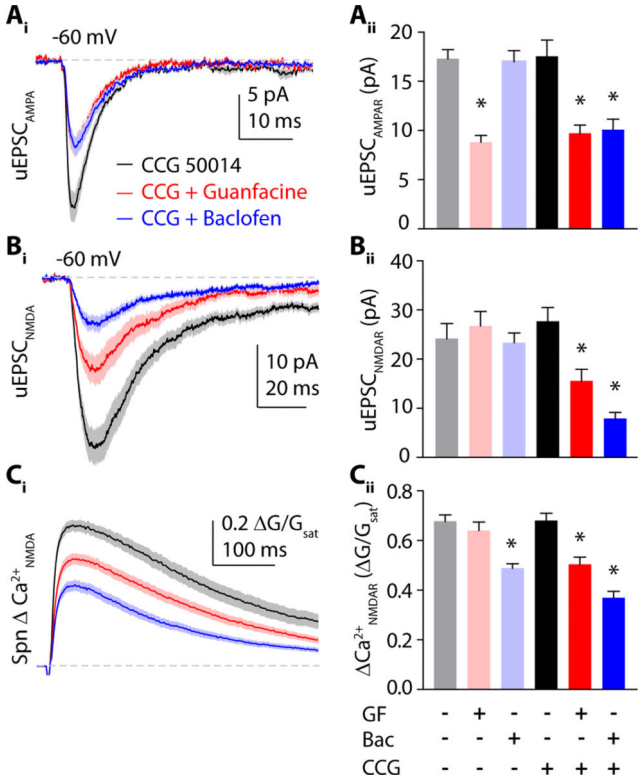

Figure 7.

Blocking RGS4 enables cross-talk between modulatory signaling pathways. (**Ai**) AMPAR-mediated currents in the presence of CCG50014 alone (black) or in combination with guanfacine (red) or baclofen (blue). (**Bi**) NMDAR-mediated currents and (**Ci**) Ca2+ transients in the presence of the RGS4 inhibitor CCG50014 either alone (black) or in combination with guanfacine (red) or baclofen (blue). Traces show mean ± SEM (solid lines and shaded areas, respectively). (**Aii**) Mean amplitude ± SEM of AMPAR-mediated currents in control (gray), guanfacine (pink) and baclofen (light blue) – reproduced from Figure 1 – or in CCG50014 (black), CCG50014 with guanfacine (red) and CCG50014 with baclofen (blue). (**Bii**) Bars represent mean amplitude ± SEM of NMDAR-mediated currents and (**Cii**) Ca2+ transients in control (gray), guanfacine (pink) and baclofen (light blue) – from Figure 1, or in CCG50014 (black), CCG50014 with guanfacine (red) and CCG50014 with baclofen (blue). *: $p<0.05$, Tukey`s multiple comparison test.